Electrochimica Acta 56 (2011) 7940–7945

Contents lists available at ScienceDirect

Electrochimica Acta

journal homepage: www.elsevier.com/locate/electacta

Electrochemical impedance study of self-assembled layer-by-layer iron–silicotungstate/poly(ethylenimine) modified electrodes

Diana M. Fernandes[a,1], Mariana E. Ghica[b,1], Ana M.V. Cavaleiro[a], Christopher M.A. Brett[b,*,1]

[a] Department of Chemistry/CICECO, University of Aveiro, 3810-193 Aveiro, Portugal
[b] Department of Chemistry, Faculty of Science and Technology, University of Coimbra, 3004-535 Coimbra, Portugal

ARTICLE INFO

Article history:
Received 29 July 2010
Received in revised form 14 January 2011
Accepted 15 January 2011
Available online 22 January 2011

Keywords:
Polyoxometalates
Poly(ethylenimine)
Self-assembly
Layer-by-layer
Electrochemical impedance spectroscopy

ABSTRACT

Electrochemical impedance spectroscopy (EIS) has been used to study multilayer films containing anionic iron-substituted silicotungstate $[SiW_{11}Fe^{III}(H_2O)O_{39}]^{5-}$ ($SiW_{11}Fe$) and positively charged poly(ethylenimine) self-assembled by the layer-by-layer method on glassy carbon and indium tin oxide electrodes. The effect of the charge of the outermost layer of the multilayer assembly on the electron transfer of soluble species was studied using the redox probes $[Fe(CN)_6]^{3-}$ and $[Ru(NH_3)_6]^{3+}$; cyclic voltammetry indicating that the surface charge has a significant effect on the process. EIS demonstrated that the electrostatic attraction or repulsion between the surface and the redox probes plays a significant role. Analysis of the impedance spectra showed that the charge transfer resistance increases with an increasing number of bilayers for both redox probes and that the porosity of the multilayer film, which varies with the electrode substrate, also has a significant effect on the electrochemical response.

1. Introduction

In recent years, many techniques have been developed to fabricate composite films since they can be used to design and build different types of molecular architectures. Layer-by-layer (LbL) assembly has proved to be a promising technique for fabricating uniform and ultrathin film devices by the alternate immersion of a substrate into solutions containing the chosen oppositely-charged species [1,2]. Film formation is attributed primarily to electrostatic interactions and van der Waals forces [1,3,4]. Functional components such as transition–metal complexes, cationic surfactants and polycations, can be assembled in an orderly fashion into multilayer films by the LbL method, which provides a high degree of control over composition, thickness, and orientation of each layer at the molecular level [1,5–7].

Among the substances that can be used in the preparation of multilayer films, polyoxometalates (POMs) deserve special attention due to their very well-defined molecular structures and to their physical and chemical properties, which makes them interesting compounds for applications in many fields such as catalysis [8,9], electrochemistry [10], materials science [11–14] and even in medicine [15]. POMs have been extensively applied in the field of chemically modified electrodes, owing to their excellent thermal and redox stability, and electrocatalytic properties. They exhibit fast reversible multiple electron redox transformations without decomposition.

Multilayers based on POMs, polyelectrolytes and conducting polymers have been widely used [16–20]. However, there are only a few reports on the characterisation of the structure and charge transfer processes in these multilayer films.

Electrochemical impedance spectroscopy (EIS) has been successfully used to study interfacial processes, in order to obtain information about the structure and changes that may occur at the electrode–electrolyte interface, and about reaction mechanisms and electrode kinetics [21]. It is an effective method to investigate the interfacial properties of modified electrodes [22–24]. EIS is complementary to cyclic voltammetry, that often allows quantitative determination of kinetic and diffusion parameters [25], and is able to study processes with time constants that vary through several orders of magnitude.

Modification of electrode substrates alters the features of impedance spectra. Impedance methods are also attractive because of the small sinusoidal potential perturbations that are used, rather than the wide potential window used in cyclic voltammetry. Thus, EIS has unique benefits for monitoring the formation processes of multilayer films and in the characterisation of the films and their interfacial properties.

In the present work, electrochemical impedance spectroscopy was used to characterise glassy carbon electrodes modified with hybrid films composed of poly(ethylenimine) and a Keggin-type polyoxometalate $[SiW_{11}Fe^{III}(H_2O)O_{39}]^{5-}$ ($SiW_{11}Fe$), using

* Corresponding author. Tel.: +351 239835295; fax: +351 239827703.
E-mail address: brett@ci.uc.pt (C.M.A. Brett).
[1] ISE member.

0013-4686/$ – see front matter © 2011 Elsevier Ltd. All rights reserved.
doi:10.1016/j.electacta.2011.01.046

$K_3[Fe(CN)_6]$ and $[Ru(NH_3)_6]Cl_3$ as redox probes. Cyclic voltammetry was also employed for characterisation. Impedance spectra were analysed by fitting to equivalent electrical circuits and the effect of the number of layers, and of the two redox probes used on the spectra and on the charge transfer processes are discussed.

2. Experimental

2.1. Reagents and solutions

The potassium salt $K_5[SiW_{11}Fe^{III}(H_2O)O_{39}]\cdot 13H_2O$ was prepared as described in the literature [26]. The compound was characterised by thermal and elemental analysis, infrared spectroscopy and powder X-ray diffraction, and the results were in agreement with previously published values [26].

Poly(ethylenimine) (PEI) (MW = 50,000–100,000; 30 wt.% aqueous solution; branched, consisting of tertiary, secondary and primary amino groups in the ratio of 25/50/25, respectively) was purchased from Polysciences Europe GmbH and was used without further treatment. Sodium chloride (Merck), potassium chloride (Merck), acetic acid (Pronalab), sodium acetate (Carlo Erba), potassium ferricyanide (Merck), hexaammineruthenium (III) chloride (Aldrich) and other reagents were analytical grade and used as received.

The electrolyte used for electrochemical studies was prepared by mixing appropriate amounts of CH_3COOH (0.1 M) and $NaCH_3COO$ (0.1 M) solutions to give a pH 4.0 solution. Potassium hexacyanoferrate (III) and hexaammineruthenium (III) solutions (1.0 mM) were prepared by dissolving the appropriate amount of $K_3[Fe(CN)_6]$ and $[Ru(NH_3)_6]Cl_3$ in 0.1 M KCl. Electrolyte solutions were prepared using ultra-pure water (resistivity 18.2 MΩ cm at 25 °C, Direct-Q 3 UV system, Millipore).

The solutions used for film assembly were used immediately after their preparation and degassed with pure nitrogen for at least 10 min.

2.2. Instrumentation and methods

A glassy carbon disc, GCE, (3.0 mm diameter, BAS, MF-2012 was used as working electrode, on which the multilayer films were formed. Indium tin oxide (ITO) electrodes with geometric area of 0.50 cm^2 (ITO on quartz slides) were also used as substrate for comparison. The auxiliary and reference electrodes were platinum wire (7.5 cm, BAS, MW-1032) and Ag/AgCl (sat. KCl) (BAS, MF-2052), respectively.

Cyclic voltammetry experiments were carried out using a computer-controlled potentiostat (PGSTAT-12/GPES software from Metrohm Autolab, The Netherlands) in a conventional three-electrode compartment cell.

Electrochemical impedance measurements were carried out using a Solartron 1250 Frequency Response Analyser, coupled to a Solartron 1286 Electrochemical Interface (UK) controlled by ZPlot Software. The voltage perturbation was 10 mV rms over a frequency range from 65 kHz to 0.01 Hz with 10 frequencies per decade, and integration time 60 s. Impedance spectra were analysed by fitting to equivalent electrical circuits using ZView Software (Scribner Associates, USA). After examination of Bode plots of the spectra, it was verified that there no hidden high frequency features, so all spectra are shown as complex plane plots.

A combined glass electrode (Hanna Instruments HI 1230) connected to an Inolab pH level 1 pH meter was used for the pH measurements.

Elemental analysis of W, Si and Fe were performed by ICP spectrometry (University of Aveiro, Central Laboratory of Analysis). Powder X-ray diffraction, thermogravimetric and FTIR studies were performed as indicated previously [27].

2.3. Preparation of self-assembled $(PEI/POM)_n$ films

Prior to coating, the GCE was conditioned by a polishing/cleaning procedure. The GCE was successively cleaned with diamond polishing compound 1.0 μm (Metadi II, Buehler) and aluminium oxide of particle size 0.3 μm (Buehler-Masterprep) on a microcloth polishing pad (BAS Bioanalytical Systems Inc.); the electrode was then rinsed with ultra-pure water and finally sonicated for 5 min in an ultrasonic bath (Branson 2510). The ITO electrodes were cleaned by placing them in a H_2SO_4/H_2O_2 (3:1) (v/v) hot bath (~80 °C) for 40 min followed by a $H_2O/H_2O_2/NH_3$ (5:1:1) (v/v/v) hot bath (~80 °C) for another 40 min. They were then rinsed with ultra-pure water and dried under a stream of pure nitrogen.

After the cleaning step, the GCE (or ITO electrode) was immersed in a 5 mg mL^{-1} PEI solution (in pH 4.0 acetate buffer) for 20 min. The electrode was then immersed in a 0.3 mM POM solution (in pH 4.0 acetate buffer) for 20 min. Water rinsing and nitrogen drying steps were performed after each immersion step. This process was repeated until the desired number of bilayers of PEI/POM was obtained. All measurements were made at room temperature (~20 °C).

3. Results and discussion

3.1. Voltammetric behaviour

Cyclic voltammetry was used to study the properties of the multilayer films towards the negatively charged $[Fe(CN)_6]^{3-}$ redox probe and the positively charged $[Ru(NH_3)_6]^{3+}$. Electrostatic attraction between the multilayer surface and the redox probe when they have opposite charges should facilitate the interfacial electron transfer process, whereas repulsion when they have the same charge would make the electron transfer reaction more difficult. Many groups have used the $[Fe(CN)_6]^{3-/4-}$ redox couple to study the permeability of multilayer films [2,28–31], but studies of electron transfer at films containing polyoxometalates are few. Liu et al. showed that the permeability could be tailored through the multilayer construction and deposition conditions [2]. Our previous studies showed how the number of layers in the films influences the shape of the cyclic voltammograms [32].

The electrochemical behaviour of the negatively charged $[Fe(CN)_6]^{3-}$ was studied at the electrode modified with $(PEI/SiW_{11}Fe)_n$ for an increasing number of bilayers (n) with the external layer being the POM. Fig. 1 shows cyclic voltammograms for an electrode with 1 and 6 bilayers. For an electrode coated with a single $(PEI/SiW_{11}Fe)$ bilayer, the cyclic voltammogram exhibits quasi-reversible properties, indicating that the probe diffuses freely through the layer to undergo electron transfer at the electrode surface. Increasing the number of bilayers from one to four leads to a decrease in peak currents and peak broadening and ultimately to a voltammogram with plateau-shaped current characteristics [32]. Thus, an increased number of multilayers with a terminal negatively-charged $SiW_{11}Fe$ anion leads to a decrease in the number of negatively charged hexacyanoferrate ions which reach the electrode substrate, attributed to electrostatic repulsion, and the process is diffusion-limited.

When the outermost layer is the positively charged PEI the quasi-reversible properties in the cyclic voltammogram of $[Fe(CN)_6]^{3-}$ are unaffected, or restored if PEI is deposited on top of a previous film structure with an external POM layer. Thus, whenever the layered film is terminated with the positively-charged PEI layer, there ceases to be any barrier to transport through the film

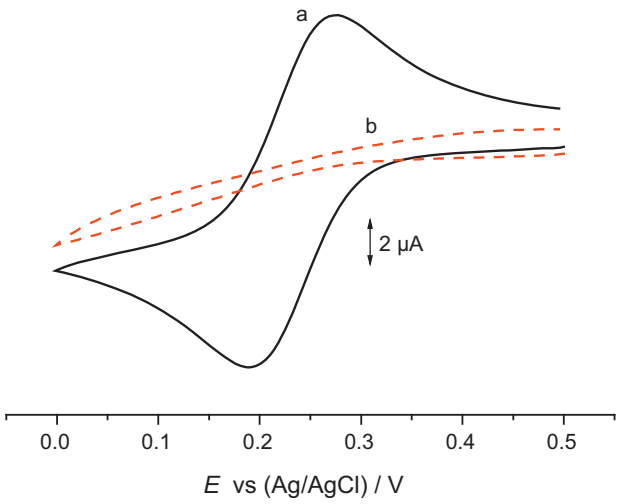

Fig. 1. Cyclic voltammograms of 1 mM $K_3Fe(CN)_6$ in 1.0 M KCl, $v = 100\,mV\,s^{-1}$ at modified electrodes with $(PEI/SiW_{11}Fe)_n$ for (a) $n = 1$ and (b) 6.

because of the electrostatic attraction of $[Fe(CN)_6]^{3-/4-}$ and the terminal positively-charged PEI layer. The voltammogram is similar to that of a bare electrode in the presence of $[Fe(CN)_6]^{3-/4-}$ species, independent of film thickness.

When the positively charged $[Ru(NH_3)_6]^{3+}$ redox probe is used, the differences observed are not so significant, see Fig. 2. The cyclic voltammograms for the first two bilayers with external layer of POM anion are almost identical; there is a slight decrease in the peak currents and an increase in the peak-to-peak separation on increasing the number of bilayers to four. However, after the addition of a layer of PEI to the $(PEI/SiW_{11}Fe)_1$ modified electrode, the peak currents of $[Ru(NH_3)_6]^{3+/2+}$ decrease significantly and peak-to-peak separation increases. This is attributable to electrostatic repulsion of $[Ru(NH_3)_6]^{3+/2+}$ by the positively-charged PEI.

The electrostatic attractions or repulsions have significant effects on the kinetics of the redox reactions. With an increasing number of (PEI/POM) bilayers the peak currents of both redox probes decrease gradually, and the peak-to-peak separation increases, indicating that the kinetics of the redox reactions become slower.

Electrochemical impedance experiments were carried out taking these cyclic voltammetry observations into account.

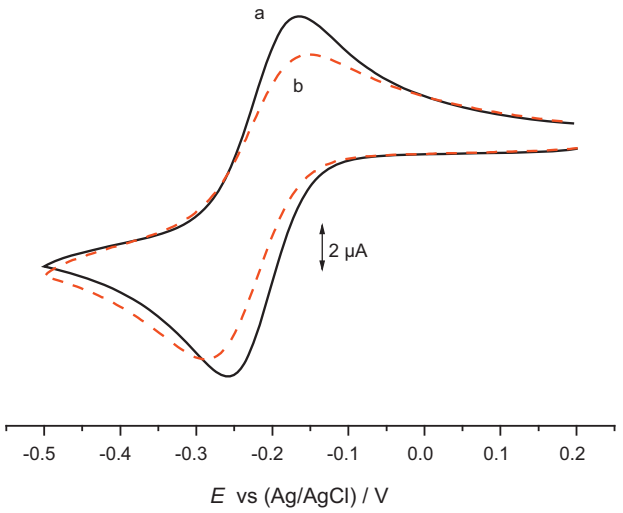

Fig. 2. Cyclic voltammograms of 1 mM $Ru(NH_3)_6Cl_3$ in 1.0 M KCl, $v = 100\,mV\,s^{-1}$ at modified electrodes with $(PEI/SiW_{11}Fe)_n$ for (a) $n = 1$ and (b) 4.

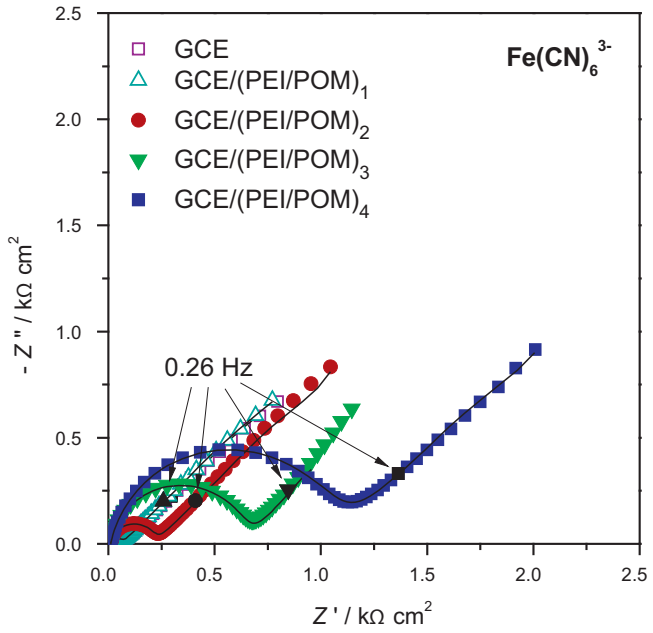

Fig. 3. Complex plane impedance spectra of different modified electrodes in the presence of 3 mM $K_3Fe(CN)_6$ in 1.0 M KCl at +250 mV vs. SCE. Lines indicate equivalent circuit fitting.

3.2. Electrochemical impedance characterisation

Electrochemical impedance spectroscopy was used to examine the electrical properties of the multilayer assembly which should change as it is built up and provide information which is complementary to that of cyclic voltammetry during the step deposition of the charged PEI and POM layers. Impedance spectra were recorded after the deposition of each layer of PEI and POM in order to investigate the effect of the structure and thickness of the multilayer on the overall interfacial properties. The experiments were done in 3 mM $K_3[Fe(CN)_6]$ and in 3 mM $[Ru(NH_3)_6]Cl_3$, both in 0.1 M KCl electrolyte, at +250 mV and −200 mV vs. SCE, respectively.

Figs. 3 and 4 show complex plane impedance spectra at glassy carbon electrodes with different numbers of PEI/POM bilayers using $[Fe(CN)_6]^{3-}$ and $[Ru(NH_3)_6]^{3+}$ redox probes, respectively. Changes can be clearly seen in the spectra during the stepwise formation of the multilayer assemblies. The impedance spectra comprise a semicircle in the high frequency range that corresponds to kinetic control of the charge-transfer process and a linear part at lower frequencies, attributable to diffusion control. The diameter of the semicircle increases with an increasing number of PEI/POM bilayers, which can be ascribed to the increase in film thickness and change in the apparent charge transfer resistance.

For the glassy carbon electrode (GCE) covered with only one layer of the positively-charged PEI, tested in $K_3Fe(CN)_6$ solution, no semicircle was observed. A similar behaviour was found for GCE and $GCE/(PEI/POM)_1$ in the solution containing $[Ru(NH_3)_6]^{3+}$. This suggests that the semicircle region is very small and the spectrum is dominated by the Warburg impedance, and thence diffusion control, over nearly the whole range of frequencies examined.

Quantitative information can be obtained by analysis using appropriate electrical equivalent circuits, Fig. 5 and extraction of the electrical parameters, as shown in Table 1. The fitting circuit in Fig. 5a is a typical Randles circuit that has been used to fit some other similar LBL-assembled structures containing POMs [33–35]. The circuit comprises a cell resistance, R_Ω, in series with a parallel combination of a constant phase element, CPE and a charge transfer resistance, R_{ct}, together with a Warburg impedance, Z_W. The CPE

Table 1
Parameters obtained from impedance spectra of the $(PEI/POM)_n$ multilayer assemblies at GCE in the presence of 3 mM $[Fe(CN)_6]^{3-}$ and 3 mM $[Ru(NH_3)_6]^{3+}$ redox probes (Figs. 3 and 4), by fitting to equivalent circuits in Fig. 5.

Redox probe	Number of bilayers	$R_{ct}/\Omega\,cm^2$	$C/\mu F\,cm^{-2}\,s^{n-1}$	n	$R_{dif}/k\Omega\,cm^2$ (W_0)
$[Fe(CN)_6]^{3-}$	0	56	6.0	0.82	3.0
	1	55	11.9	0.86	2.9
	2	210	6.8	0.80	2.9
	3	643	7.2	0.83	1.6
	4	1056	9.5	0.81	3.5
$[Ru(NH_3)_6]^{3+}$	0	–	–	–	1.7
	1	–	–	–	1.6
	2	11.0	106	0.67	1.2
	3	14.9	69	0.69	1.3
	4	32.1	140	0.65	1.2

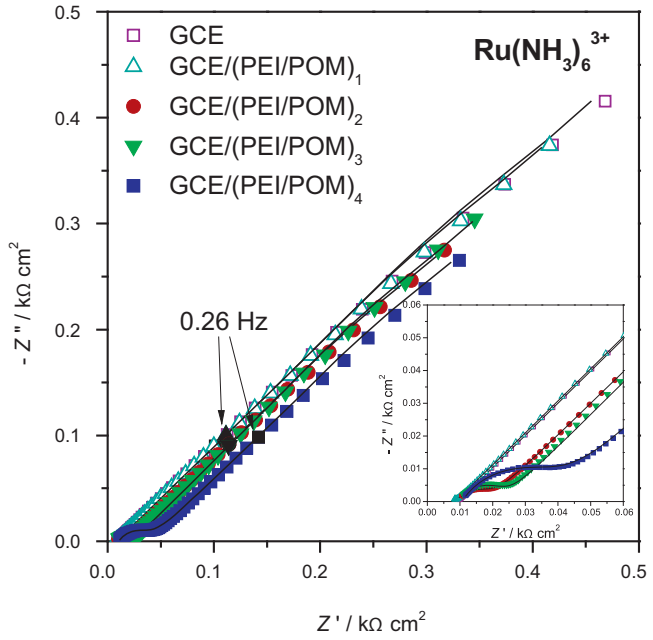

Fig. 4. Complex plane impedance spectra of different modified electrodes in the presence of 3 mM $Ru(NH_3)_6Cl_3$ in 1.0 M KCl at −200 mV vs. SCE. In the inset is a magnification of the high frequency part of the spectra. Lines indicate equivalent circuit fitting.

was modelled as a non-ideal capacitor, given by $CPE = -1/(Ci\omega)^n$, where C is the capacitance, which describes the charge separation at the double layer interface, ω is the frequency in rad s^{-1} and the n exponent is due to the heterogeneity of the surface. The Warburg impedance was modelled as an open circuit finite Warburg element which includes a diffusion resistance, R_{dif}, according to

$$Z_W(W_o) = \frac{R_{dif}\,ctnh([i\tau\omega]^{\alpha})}{(i\tau\omega)^{\alpha}} \quad (1)$$

where R_{dif} is the diffusion resistance of electroactive species, τ a time constant depending on the diffusion rate ($\tau = l^2/D$, where l is the effective diffusion thickness, and D is the effective diffusion coefficient of the species), and $\alpha = 0.5$ for a perfect uniform flat interface. The circuit in Fig. 5b is a simplified version of that in Fig. 5a, comprising the cell resistance and the Warburg element, used where no semicircle appeared. The cell resistance, R_Ω, is $9.7 \pm 0.5\,\Omega\,cm^2$ in all cases at the GCE and the Warburg element exponent, α, was always close to 0.50, see Table 1.

Fig. 6a and b shows plots of the values of charge transfer resistance for both redox probes at the bare electrode and for $(PEI/SiW_{11}Fe)_n$ multilayers (n = 1–4). The circuit element of most interest is R_{ct} because it can be related directly to the access to the substrate in the modified GCE electrode, where electron transfer of the electroactive species in solution occurs.

Considering hexacyanoferrate (III) anion, Fig. 6a, with just one $(PEI/SiW_{11}Fe)$ bilayer assembled on the electrode, R_{ct} is almost the same as at the bare electrode, which indicates that the probe is able to diffuse easily through the bilayers, despite the probe and outer layer having the same charge, and undergo electron transfer at the electrode surface. This is in agreement with cyclic voltammetry that showed a quasi-reversible cyclic voltammogram for $(PEI/SiW_{11}Fe)_1$. As the number of layers increases, as well as the thickness of the multilayer structure, the difficulty of reaching the electrode substrate becomes significantly more pronounced, in a non-linear fashion, indicating a multilayer structure with fewer pores that traverse the film. Assuming that this model is correct, comparing with the bare electrode/one-bilayer system the increase in apparent charge transfer resistance implies a reduction in accessible substrate surface area down to 27% (2 bilayers) 9% (3 bilayers) and 5% (4 bilayers). This agrees with other results in the literature, e.g. [36], which suggest that the coverage of the surface by self-assembly is not usually perfect and such defects are progressively removed as the number of bilayers is increased. Interestingly, the values of capacitance are relatively small and change little as do the values of the CPE exponent at around 0.8.

For the ruthenium (III) electroactive species, the values of R_{ct} are, in general, more than an order of magnitude lower than for hexacyanoferrate (III), compare Figs. 6a and b. For zero or one bilayers, there is no measurable apparent charge transfer resistance, the process being entirely controlled by diffusion. Resistance to charge transfer only becomes evident for 2 and more bilayers, supporting this explanation. When access does become physically limited, for 2 or more bilayers, it is still much easier than with hexacyanoferrate (III), as would be expected, and charge separation is much greater, with capacitance values an order of magnitude higher. The diffusion resistance values are correspondingly lower. Nevertheless, the CPE exponent is also lower suggesting that non-

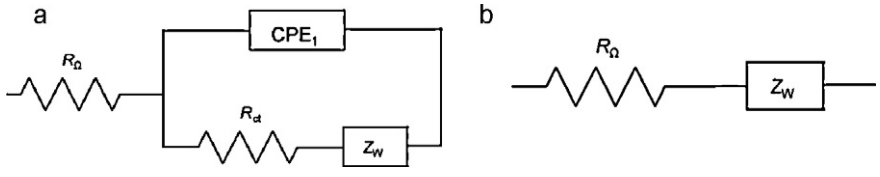

Fig. 5. Equivalent electrical circuits used to fit the impedance spectra.

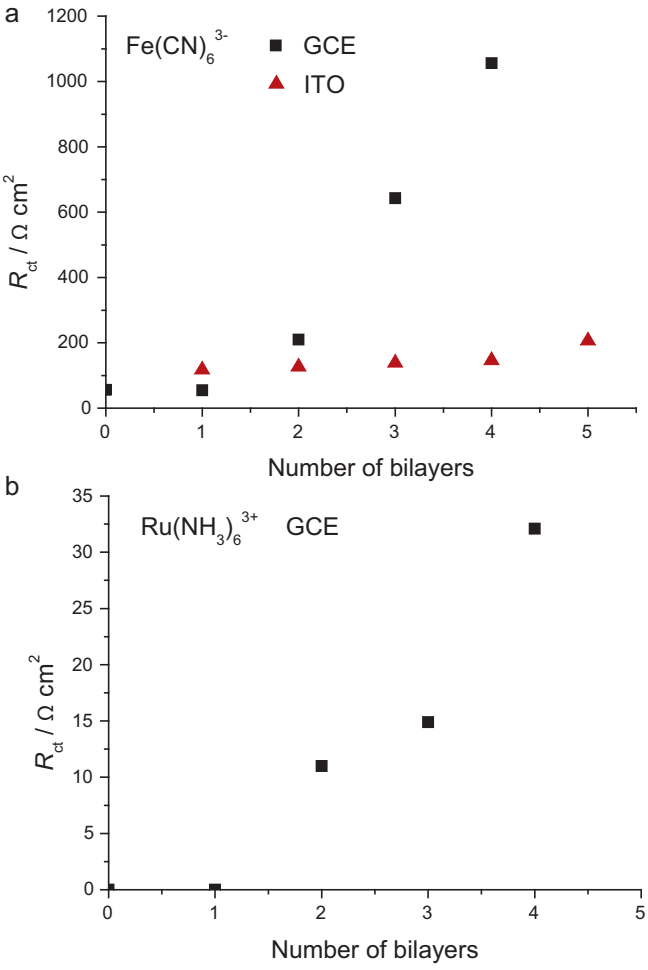

Fig. 6. Plots of R_{ct} vs. the number of layers of $(PEI/POM)_n$ multilayer assemblies in the presence of (a) 3 mM $K_3Fe(CN)_6$ for GCE (■) and ITO electrodes (▲) (b) 3 mM $Ru(NH_3)_6Cl_3$ for GCE. Data from Tables 1 and 2.

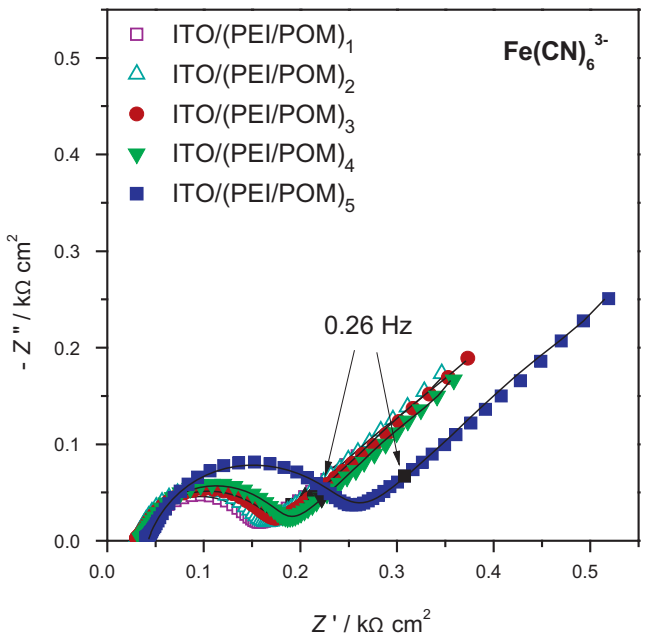

Fig. 7. Complex plane impedance spectra of different ITO modified electrodes in the presence of 3 mM $K_3Fe(CN)_6$ in 0.1 M KCl at 250 mV vs. SCE. Lines indicate equivalent circuit fitting.

Table 2
Parameters obtained from impedance spectra of the $(PEI/POM)_n$ multilayer assemblies at ITO electrodes in the presence of 3 mM $[Fe(CN)_6]^{3-}$ redox probe (Fig. 7) by fitting to the equivalent circuit in Fig. 5a.

Number of bilayers	$R_{ct}/\Omega\,cm^2$	$C/\mu F\,cm^{-2}\,s^{n-1}$	n	$R_{dif}/k\Omega\,cm^2$ (W_0)
1	117	65	0.82	0.47
2	126	29	0.86	0.66
3	138	60	0.80	0.79
4	146	57	0.83	0.61
5	206	50	0.81	0.97

uniformities in the surface play a much larger role when the sign of the charges of the electroactive species and the outermost layer are opposite, the effect of surface roughness having greater influence on species transport. Such highly non-uniform surfaces, when the outermost layer is POM, have been demonstrated by scanning electron microscopy in [32].

Analysis of the spectra for these two redox species clearly demonstrates that the electrostatic attraction or repulsion between the redox probe and the surface of the multilayer assemblies plays a significant role in the charge transfer process, repulsion for $[Fe(CN)_6]^{3-/4-}$ and attraction for $[Ru(NH_3)_6]^{3+/2+}$, with the negatively-charged layer of POM. On the other hand, the adsorption of the next layer, positively charged PEI, reverses the surface charge and the electrostatic interaction creates attraction of the negatively charged $[Fe(CN)_6]^{3-/4-}$ and repulsion of the positively charged $[Ru(NH_3)_6]^{3+/2+}$, leading to higher charge transfer resistances for the $[Ru(NH_3)_6]^{3+}$ redox probe (data not shown).

The impedance spectra for electrodes terminated with a PEI layer, tested with both redox probes, were also recorded and present the same general features as those terminated with a POM layer, and the conclusions with respect to the signs of the positive charge on the PEI layer and the charge of the redox probe are the same, so are not further discussed here.

Comparative experiments using $[Fe(CN)_6]^{3-}$ were carried out on indium tin oxide electrode substrates on which multilayer films were formed, in order to assess the influence of the electrode substrate, see Fig. 7. The same trends were observed with respect to different numbers of bilayers as at glassy carbon, see Table 2 and Fig. 6a. However, although an increased number of bilayers leads to higher values of the apparent charge transfer resistance, the values, which are initially larger than at glassy carbon electrodes by a factor of two, increase less, less than doubling after 5 bilayers. This suggests that the deposition through layer-by-layer self-assembly is occurring in a different way and the identity of the substrate is important. In particular, there is evidence that imperfections due to incomplete coverage on parts of the substrate surface which are not covered by the first bilayers continue. Finally, the values of the capacitance are much higher than at glassy carbon electrodes and the diffusion resistance is lower, giving indications that the multilayer also has a different internal structure.

4. Conclusions

The present work has demonstrated that the behaviour of self-assembled multilayer films in the presence of redox probes can be successfully investigated using electrochemical impedance spectroscopy. In particular, the charge transfer reactions at the surface of a $(PEI/POM)_n$ modified electrode can be affected by the thickness of the multilayer assembly and by the electrostatic attraction and repulsion between the surface of the assembly and the electroactive species in solution. With the negatively charged hexacyanoferrate (III), the outermost negatively-charged POM anion leads to electrostatic repulsion as well as less penetration through to the

electrode surface, which causes the apparently higher charge transfer resistance observed. If another layer (PEI) is deposited so that the outermost layer is positively charged, this resistance becomes lower again. The opposite is true with the positively charged hexammineruthenium (III) species.

EIS is able to show differences between layer-by-layer assemblies more clearly than cyclic voltammetry. Impedance spectra are sensitive to, and can distinguish between, multilayer construction on different substrates, as seen with glassy carbon and indium tin oxide, and also give information on surface non-uniformity and defects in the first adsorbed layers. Thus, the use of EIS constitutes an important approach to investigate LbL modified electrodes, which are receiving increasing attention, as is their application in sensors and biosensors.

Acknowledgments

Financial support from Fundação para a Ciência e a Tecnologia (FCT), POCI/QUI/56534/2004 and PTDC/QUI/65732/2006 POCI 2010 (co-financed by the European Community Fund FEDER), CICECO, the University of Aveiro and CEMUC® (Research Unit 285), Portugal, is gratefully acknowledged. FCT is also thanked for a PhD grant for DMF (SFRH/BD/30797/2006) and a postdoctoral fellowship grant for MEG (SFRH/BPD/36930/2007).

References

[1] G. Decher, Science 277 (1997) 1232.
[2] S. Liu, D.G. Kurth, B. Bredenkotter, D. Volkmer, J. Am. Chem. Soc. 124 (2002) 12279.
[3] P. Bertrand, A. Jonas, A. Laschewsky, R. Legras, Macromol. Rapid Commun. 21 (2000) 319.
[4] F.N. Crespilho, V. Zucolotto, O.N. Oliveira Jr., F.C. Nart, Int. J. Electrochem. Sci. 1 (2006) 194.
[5] D.G. Kurth, D. Volkmer, M. Ruttorf, B. Richter, A. Müller, Chem. Mater. 12 (2000) 2829.
[6] P.J. Kulesza, M. Chojak, K. Miecznikowski, A. Lewera, M.A. Malik, A. Kuhn, Electrochem. Commun. 4 (2002) 510.
[7] D. Ingersoll, P.J. Kulesza, L.R. Faulkner, J. Electrochem. Soc. 141 (1994) 140.
[8] C.L. Hill, C.M. Prosser-McCartha, Coord. Chem. Rev. 143 (1995) 407.
[9] B. Keita, L. Nadjo, J. Mol. Catal. A: Chem. 262 (2007) 190.
[10] D.E. Katsoulis, Chem. Rev. 98 (1998) 359.
[11] M.T. Pope, A. Müller, Angew. Chem. Int. Ed. 30 (1991) 34.
[12] J.M. Clemente-Juan, E. Coronado, Coord. Chem. Rev. 193 (1999) 361.
[13] P. Gomez-Romero, Adv. Mater. 13 (2001) 163.
[14] E. Coronado, C. Giménez-Saiz, C.J. Gómez-Garcia, Coord. Chem. Rev. 249 (2005) 1776.
[15] J.T. Rhule, C.L. Hill, D.A. Judd, Chem. Rev. 98 (1998) 327.
[16] M. Skunik, B. Baranowska, D. Fattakhova, K. Miecznikowski, M. Chojak, A. Kuhn, P.J. Kulesza, J. Solid State Electrochem. 10 (2006) 168.
[17] P.J. Kulesza, M. Skunik, B. Baranowska, K. Miecznikowski, M. Chojak, K. Karnicka, E. Frackowiak, F. Béguin, A. Kuhn, M. Delville, B. Starobrzynska, A. Ernst, Electrochim. Acta 51 (2006) 2373.
[18] D. Fan, J. Hao, J. Phys. Chem. B 113 (2009) 7513.
[19] B. Xu, L. Xu, G. Gao, W. Guo, S. Liu, J. Colloid Interface Sci. 330 (2009) 408.
[20] S. Gao, R. Cao, C. Yang, J. Colloid Interface Sci. 324 (2008) 156.
[21] C.M.A. Brett, A.M. Oliveira Brett, Electrochemistry, Principles Methods and Applications, 11, Oxford University Press, Oxford, 1993 (Chapter 11).
[22] H.O. Finklea, D.A. Snider, J. Fedyk, E. Sabatani, Y. Gafni, I. Rubinstein, Langmuir 9 (1993) 3660.
[23] H. Taira, K. Nakano, M. Maeda, M. Takagi, Anal. Sci. 9 (1993) 199.
[24] A. Bardea, F. Patolsky, A. Dagan, I. Willner, Chem. Commun. (1999) 21.
[25] A.J. Bard, L.R. Faulkner, Electrochemical Methods: Fundamentals and Applications, Wiley, New York, 2001.
[26] F. Zonnevijlle, C.M. Tourne, G.F. Tourne, Inorg. Chem. 21 (1982) 2751.
[27] J.A.F. Gamelas, A.M.V. Cavaleiro, E.M. Gomes, M. Belsley, E. Herdtweck, Polyhedron 21 (2002) 2537.
[28] J.J. Harris, M.L. Bruening, Langmuir 16 (2000) 2006.
[29] V. Pardo-Yissar, E. Katz, O. Lioubashevski, I. Willner, Langmuir 17 (2001) 1110.
[30] J. Dai, A.W. Jensen, D.K. Mohanty, J. Erndt, M.L. Bruening, Langmuir 17 (2001) 931.
[31] S. Gao, T. Li, X. Li, R. Cao, Mater. Lett. 60 (2006) 3622.
[32] D.M. Fernandes, H.M. Carapuça, C.M.A. Brett, A.M.V. Cavaleiro, Thin Solid Films 518 (2010) 5881.
[33] S. Zhai, S. Gong, J. Jiang, S. Dong, J. Li, Anal. Chim. Acta 486 (2003) 85.
[34] Z. Cheng, L. Cheng, Q. Gao, S. Dong, X. Yang, J. Mater. Chem. 12 (2002) 1724.
[35] G. Yang, H. Guo, M. Wang, M. Huang, H. Chen, B. Liu, S. Dong, J. Electroanal. Chem. 600 (2007) 318.
[36] C. Picart, Ph. Lavalle, P. Hubert, F.J.G. Cuisinier, G. Decher, P. Schaaf, J.C. Voegel, Langmuir 17 (2001) 7414.